Hybrid algorithm

for inverse DC/AC resistivity logging measurement simulations

***M. Paszyński[1], E. Gajda-Zagórska[1], M. Smołka[1], R. Schaefer[1], D. Pardo[2]**

[1]AGH University of Science and Technology, Krakow, Poland.
[2]The University of the Basque Country, UPV/EHU and Ikerbasque, Bilbao, Spain.

*Corresponding author: maciej.paszynski@AGH.EDU.PL

Abstract

We present a hybrid algorithm for solving inverse 3D resistivity logging measurement simulation problem with DC and AC tools in deviated wells. The term "simulation of measurements" is widely used by the geophysical community. A quantity of interest, voltage, is measured at a receiver electrode located in the logging instrument. Computer simulations are used to explain obtained measurements. We solve the inverse problem with goal-oriented *hp* adaptive finite element method interfaced with Hierarchic Genetic Strategy (HGS) algorithm during a global phase and Conjugated Gradient (CG) algorithm in a local phase. The global search HGS algorithm generates starting points for local search CG algorithm. We conclude the presentation with numerical experiments for DC/AC problems.

Keywords: inverse algorithms, resistivity logging measurement simulations, goal-oriented hp adaptive finite element method, hierarchic genetic search

Introduction

In this paper, we solve a forward and inverse problem of 3D direct and alternate current (DC/AC) borehole resistivity measurement simulations in a deviated well.

The expression "simulation of measurements" is widely used within the geophysical community. A quantity of interest, voltage in this case, is measured at a receiver electrode located in the logging instrument. Actual logging instruments are equipped with several transmitter and receiver electrodes. These instruments move along the axis of the borehole, and measure the voltage induced at the receiver electrodes at different positions. The voltage measured at the receivers is expected to be related to the electrical conductivity of the nearby formation. Thus, logging instruments are used to estimate the properties (in this case, the electrical conductivity) of the sub-surface material, with the ultimate objective of describing hydrocarbon (oil and gas) bearing formations.

In the forward problem, the behavior of a resistivity logging instrument is simulated by performing computer-based simulations of resistivity logging instruments in a borehole environment. The resulting simulator is utilized as a core part of an inverse problem infrastructure. The inverse infrastructure allows to determine unknown conductivities of formation layers, based on actual measurements recorded by logging instruments.

The resistivity logging tool with receiver and transmitter electrodes is moving along the trajectory of the well. The electromagnetic waves generated by the transmitter electrode are reflected from formation layers and recorded by the receiver electrodes. Of particular interest to the oil industry are 3D simulations of resistivity measurements in deviated wells, where the angle between the borehole and the formation layers is not equal to 90 degrees ($\theta_0 \neq 90°$).

Formulation of 3D DC/AC problem in deviated well with Fourier series expansions

A forward DC problem is formulated in the following way, by the conductive media equation:
Find $u: R^3 \supset \Omega \ni x \to u(x) \in R$ the electrostatic scalar potential such that

$$-\sum_{i=1}^{3} \sigma \frac{\partial^2 u}{\partial x_i^2} = \nabla \circ J \text{ in } \Omega \tag{1}$$

where $\nabla \circ J$ is the load (divergence of the impressed current, Pardo et al. 2006) and σ represents the conductivity of the media.

To solve the above 3D problem (1), a new quasi-cylindrical non-orthogonal system of coordinates shown in Figure 1 is introduced. This chapter presents a summary of the derivation presented in details in (Pardo et al. 2008a and Pardo et al. 2008b). The notation from the papers is utilized here. The variational formulation, with respect to the electric potential *u* in this new system of coordinates, can be expressed in the following way:

Find $u \in V$ such that:

$$\int_{\Omega} \sum_{n=1}^{3} \frac{\partial u}{\partial \zeta_n} \hat{\sigma} \frac{\partial v}{\partial \zeta_n} d\zeta = \int_{\Omega} v \nabla \circ \hat{J} \, d\zeta \quad \forall v \in V \tag{2}$$

where

$$V = \left\{ v \in L^2(\Omega) : \int_{\Omega} \|v\|^2 + \|\nabla v\|^2 \, dx < \infty : \text{tr}(v) = 0 \text{ on } \Gamma_D \right\} \tag{3}$$

The electric conductivity of media in the new system of coordinates is equal to $\hat{\sigma} := Jac^{-1} \sigma \, Jac^{-1^T} |Jac|$, and $\nabla \circ \hat{J} := \nabla \circ J |Jac|$ with *Jac* being the Jacobian matrix of the change of coordinates with respect to the Cartesian reference system of coordinates (x_1, x_2, x_3), namely,

$$Jac = \frac{\partial(x_1, x_2, x_3)}{\partial(\zeta_1, \zeta_2, \zeta_3)} \tag{4}$$

Then, we take a Fourier series expansion of the solution, material and ζ_2 direction

$$u(\zeta_1, \zeta_2, \zeta_3) = \sum_{l=-\infty}^{l=+\infty} u_l(\zeta_1, \zeta_3) e^{jl\zeta_2} \tag{5}$$

$$\sigma(\zeta_1, \zeta_2, \zeta_3) = \sum_{m=-\infty}^{m=+\infty} \sigma_m(\zeta_1, \zeta_3) e^{jm\zeta_2} \tag{6}$$

$$\nabla \circ J(\zeta_1, \zeta_2, \zeta_3) = \sum_{l=-\infty}^{l=+\infty} \nabla \circ J_l(\zeta_1, \zeta_3) e^{jl\zeta_2} \tag{7}$$

where

$u_l = \frac{1}{2\Pi} \int_0^{2\Pi} u e^{-jl\zeta_2} d\zeta_2$, $\sigma_m = \frac{1}{2\Pi} \int_0^{2\Pi} \sigma e^{-jm\zeta_2} d\zeta_2$, $\nabla \circ J_l = \frac{1}{2\Pi} \int_0^{2\Pi} f e^{-jl\zeta_2} d\zeta_2$ and *j* is the imaginary unit. We introduce symbol F_l such that applied to a scalar function *u* it produces the l^{th} Fourier modal coefficient u_l, and when applied to a vector or matrix, it produces a vector or matrix of the components being l^{th} Fourier modal coefficients of the original vector or matrix components.

Using the Fourier series expansions we get the following variational formulation:

Find $F_l(u) \in V$ such that:

$$\int_{\Omega} \sum_{l,m=-\infty}^{+\infty} F_l\left(\frac{\partial u}{\partial \xi}\right) F_m(\hat{\sigma}) \frac{\partial v}{\partial \xi} e^{j(l+m)\zeta_2} \, d\zeta = \int_{\Omega} v F_l(\hat{f}) e^{jl\zeta_2} \, d\zeta \quad \forall v \in V \tag{8}$$

The summation is applied with respect to $-\infty \le l, m \le \infty$. We select a mono-modal test function $v = v_k e^{jk\zeta_2}$.

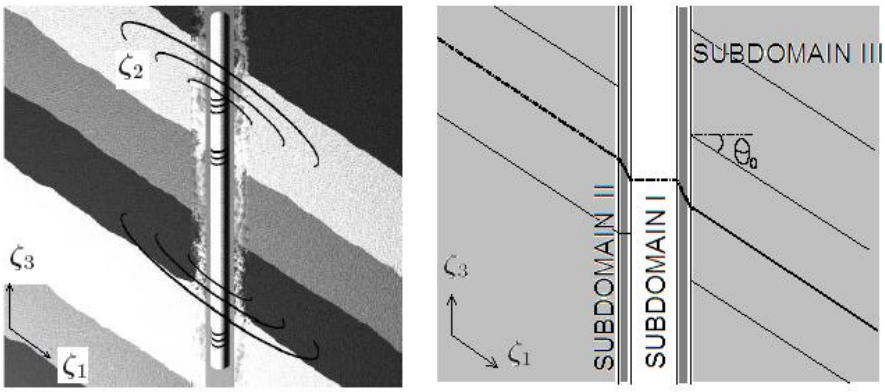

Fig. 1. Three non-orthogonal systems of coordinates in the borehole and formation layers

Thanks to the orthogonality of the Fourier modes in $L^2(\Omega)$ the problem (8) reduces to:
Find $F_l(u) \in V$ such that:

$$\int_{\Omega_{2D}} \sum_{n=k-2}^{n=k+2} F_l\left(\frac{\partial u}{\partial \xi}\right) F_{k-l}(\hat{\sigma}) F_l\left(\frac{\partial v}{\partial \xi}\right) d\zeta_1 d\zeta_3 = \int_{\Omega_{2D}} F_k(v) F_k\left(\hat{f}\right) d\zeta_1 d\zeta_3 \quad \forall F_k(v) \in V \tag{9}$$

since five Fourier modes are enough to represent exactly the new material coefficients. We refer to Pardo et al. 2008a for more details.

In the similar (however more algebraically complicated) manner, the variational formulation for the AC problem can be derived, which is presented in Pardo et al. 2008b. The forward problem is solved with self-adaptive, goal-oriented *hp* finite element method (*hp*-FEM) (Demkowicz 2006). The algorithm starts with an initial mesh, called the *coarse mesh* and solves the weak problem. The mesh is then globally *hp*-refined, each element is broken into four elements and the polynomial order of approximation is increased by one. The resulting mesh is called the *fine mesh*. The weak problem is solved again over the fine mesh. The algorithm considers different refinement strategies for each finite element from the coarse mesh.

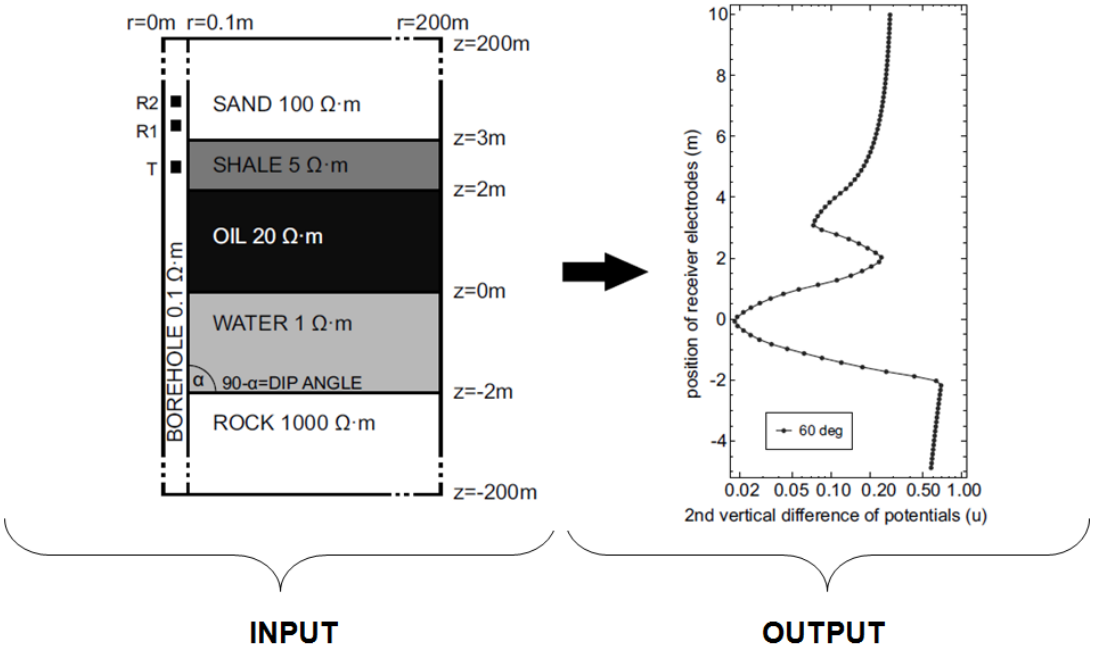

Fig. 2. The summary of the formulation of the forward problem

Forward and inverse problems

In the forward problem the behavior of resistivity logging instrument is analyzed by performing computer-based simulations for borehole environment. In particular, given the resistivities of the formation layers, the voltage at certain positions of transmitter and receiver electrodes is sought according to (9). A series of forward problems for these positions forms a *logging curve* (Figure 2). In the inverse problem (Figure 3), we are given a reference logging curve and aim to find the best approximation of the unknown resistivities that result in a curve closest to the reference one.

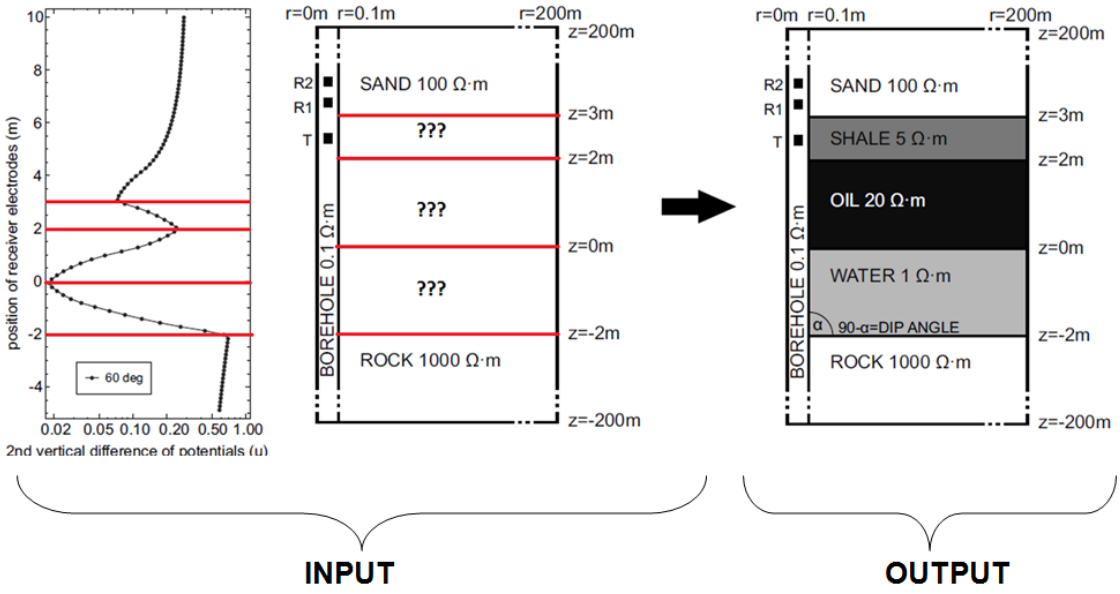

Fig. 3. The summary of the formulation of the inverse problem

Hierarchic genetic strategy interfaced with self-adaptive hp-FEM

The *hp*-HGS strategy is based on HGS (see e.g. Schaefer and Kołodziej 2004), which is dedicated to solving multimodal, global optimization problems. It creates a tree of demes, in which the encoding accuracy grows with the distance from the root. We start with most coarse, chaotic solutions (which, as a result, can be computed quickly) and as we progress down the tree, we obtain more accurate solutions, with the final ones reached in the tree leaves. In the left part of Figure 4, the individuals of the root-node deme are marked by red points. In the left and central parts, green points denote second-level (branch) individuals. For evaluation of individuals from particular levels of the tree of populations the self-adaptive hp-FEM code is used. The accuracy of the *hp*-FEM solver grows with the depth of the tree of populations. In other words, close to the root we evaluate individuals by using cheap low accuracy solver, while at the leaves of the tree of populations we utilize high accuracy expensive estimates.

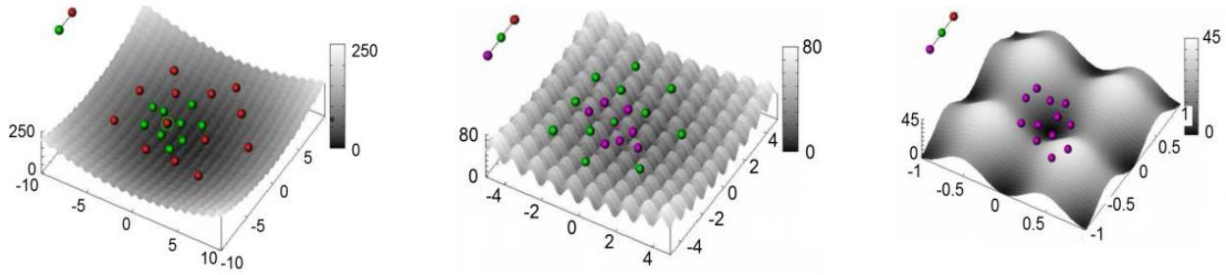

Fig. 4: Red color – root individuals, green – branch individuals, violet – leaf individuals.

The following pseudocode shows main ideas of *hp*-HGS (including scaling errors):

```
Inverse analysis loop
  do
    Solve the problem on the current coarse and fine FE mesh
    Compute FE error
    Compute goal function error on the coarse mesh
    if goal function error on the coarse mesh <
       < rate * relative FE error then
      Execute one step of (parallel) hp adaptivity
    else break endif
  enddo
  Compute goal function error on the fine mesh
  if goal function error on the fine mesh <
     < required accuracy then
    stop
  endif
  Propose new values for inverse problem parameters
endloop
```

Numerical results for pure hp-HGS algorithm

The hp-HGS algorithm has been executed for DC and AC cases. For the DC case, the algorithm has been looking for the resistivities (1,5,20) (compare Figures 2 and 3) of the three formation layers. The algorithm has found $\omega_0 \approx 1$ (correct result) and $\omega_1 \approx 5$ (correct result), however ω_2 had different values varying from 10 up to 100. The results are summarized in Figure 5; they suggest the insensitivity of the measurements to the third parameter.

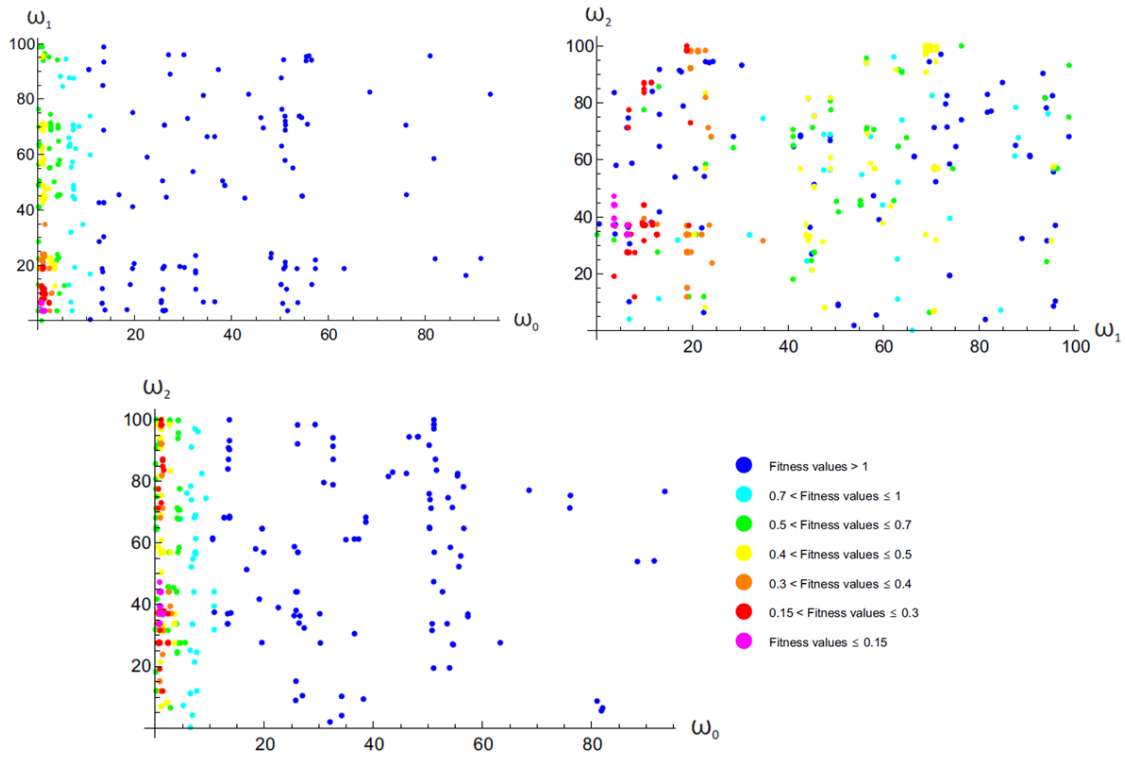

Fig. 5. The DC results of the hp-HGS algorithm

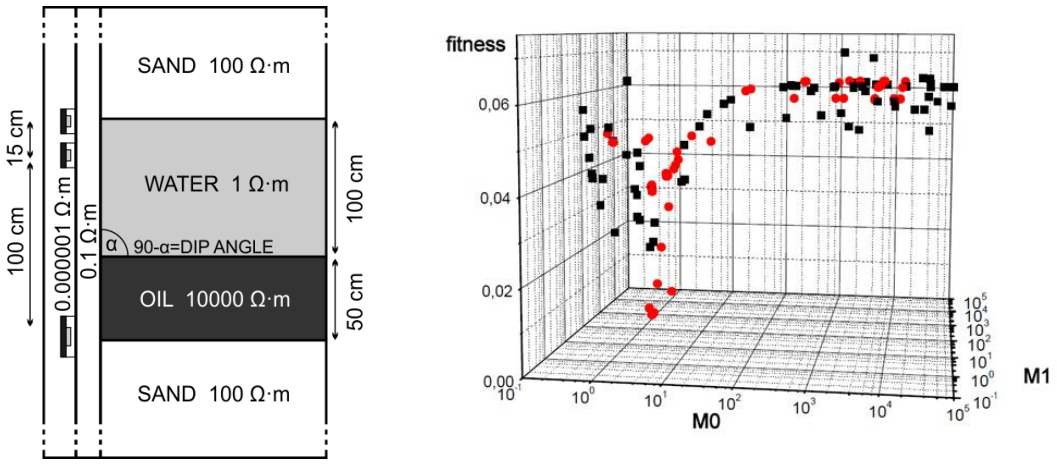

Fig. 6. The AC forward problem and inverse results of the hp-HGS algorithm

For the AC case, we solved a much more computationally difficult problem where the borehole is equipped with steel casing with high contrast resistivity (compare left panel in Figure 6). The inverse algorithm has been looking for the two central resistivities (1,10000). The algorithm has found $\omega_o \approx 1$ (correct result), however ω_1 had different values varying from 40 up to 40000. The results are summarized on the right panel in Figure 6; they suggest the insensitivity of the measurements to the second parameter.

The pure hp-HGS algorithm is suitable for recognizing the landscape of the solved problems, in particular for finding the basins of attraction of global and local minimizers in case of multimodal problems (see Schaefer and Telega 2007 and references therein). It is also capable of finding the solutions (its asymptotic properties has been formally proven), but has to be synchronized at the end of each metaepoch to determine, in which regions new branches and leaves should be sprouted. One should also notice that with increasing depth in the HGS tree, the accuracy and computation time of each candidate solution also increases, which makes the leaves the most heavy parts of the computations, even if leaf populations are very small. Summing the above facts with the stochastic nature of HGS opens the area for improvement by limiting the depth of the HGS tree and by applying local methods in the interesting regions found by hp-HGS.

Numerical results for the hybrid computations

In order to reduce the computational cost of the inverse algorithm we have interfaced the hp-HGS algorithm with conjugated gradient (CG) type of iterative method. Once the inverse algorithm finds areas with local minima, we to switch to local gradient search methods with higher accuracy.

In the DC case, we stopped the first phase hp-HGS genetic search after 6 metaepochs, when we could select six starting points for the second gradient phase from the leaves of the tree of populations. We have executed the CG algorithm from these points, with the following results:

- The CG algorithm starting from the first point and the fourth point converges to the border of the domain and gets stuck there.
- The CG algorithm starting from the second, third and the fifth point converged to local minima
- The computations started from the sixth starting point require much more iterations, and has been stopped.

The convergence history for the second, third and fifth points is presented in Figure 7.

We obtained similar results to those obtained from the global genetic search, namely $\omega_o \approx 1$ (correct result) and $\omega_1 \approx 5$ (correct result), however ω_2 had different values varying from 30 up to 60. This confirmed our thesis that these measurements are insensitive to the third layer.

In the AC case, we stopped the first phase hp-HGS genetic search after eight metaepochs and selected 10 starting points to the second phase of gradient search. All the points converged to local minima (summarized in Figure 8). We obtained similar results as those of the global genetic search, namely the algorithm has found $\omega_o \approx 1$ (correct result), however ω_1 had different values varying from 6 up to 52000. This confirmed our thesis that these measurements are insensitive to the second layer.

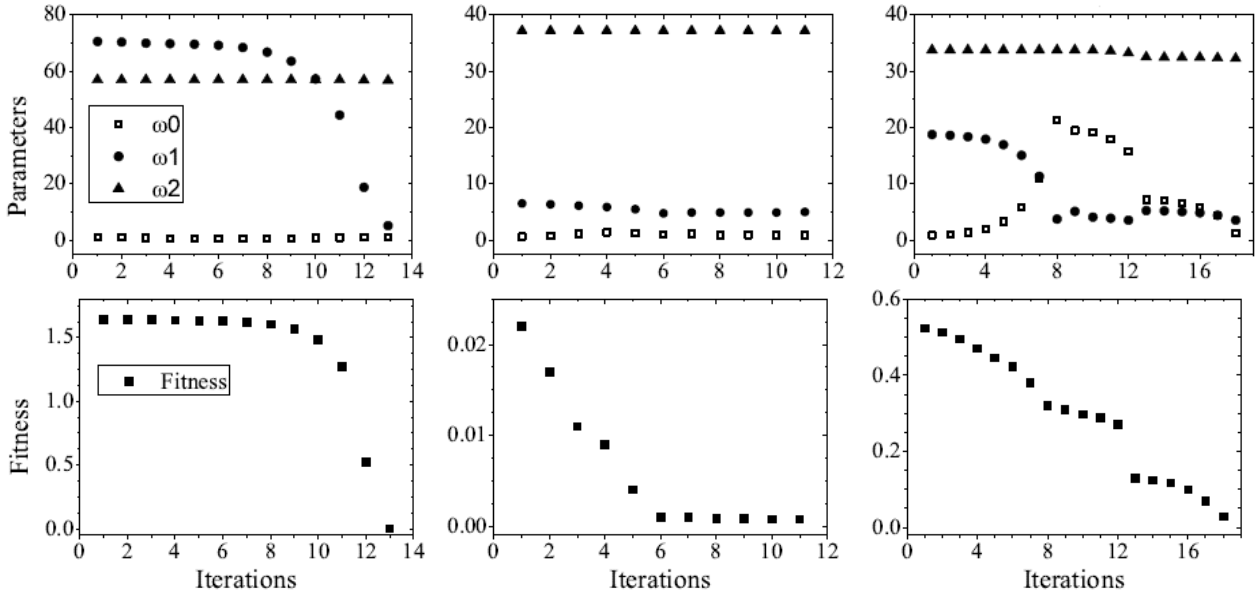

Fig. 7. The local gradient search for the DC problem

	number of solver calls	final value ω_0	final value ω_1	final fitness
1	4	1.077	542.599	0.000008582
2	61	1.234	47541.290	0.000067900
3	28	1.015	1309.719	0.000000366
4	4	1.122	74.889	0.000018307
5	8	1.038	10.406	0.000024504
6	4	0.784	769.435	0.000096289
7	4	0.798	51924.700	0.000082576
8	4	1.427	5536.764	0.000185538
9	4	0.731	124.052	0.000163327
10	24	1.242	6.815	0.000079457

Fig. 8. The local gradient search for the AC problem

Computational cost

In the DC case, the HGS algorithm finds six starting points for gradient algorithm with 5-11 genetic steps, and the gradient algorithm converges to local minima between 12-14 iterations (compare Figure 7). Thus, the local minima can be found with 17-25 direct problem evaluations.

In the AC case, the HGS algorithm finds ten starting points for gradient algorithm with 8 genetic steps, and the gradient algorithm converges to local minima with 4-28 solver calls (compare Figure 8, with the assumption that we skip the expensive second point). Thus, the local minima can be found with 12-36 direct problem evaluations.

The hybrid algorithm can be parallelized on the level of these meta-steps. Thus, the sequential execution time is equal to 17-25 or 12-36 consecutive direct solver calls, for DC or AC case, respectively.

Conclusions

In this paper we presented *hp*-HGS hierarchic genetic strategy using the self-adaptive *hp* finite element as direct solver. The *hp*-HGS was interfaced with local gradient search, which is more efficient once the genetic algorithm reaches the local minima. The strategy was utilized for solution of the inverse problem related to the identification of the formation layers based on the borehole resistivity logging measurement for direct current as well as alternate current (DC/AC) cases. In both cases the numerical results converged to a local valley, where one of the formation layers had different values. These results imply that, in some cases, the resistivity measurements are insensitive to some formation layers, and for better results they might be combined with other methods of measurements, using e.g. sonic or nuclear tools.

Acknowledgements

This work was supported by Polish National Science Center grant no. DEC-2012/05/N/ST6/03433.

References

Demkowicz, L. (2006) *Computing with hp-Adaptive Finite Element Method. Vol. I. One and Two Dimensional Elliptic and Maxwell Problems*. Chapmann & Hall / CRC Applied Mathematics and Nonlinear Science

Pardo, D. Demkowicz, L. Torres-Verdin, C. Paszyński M. (2006) Simulation of Resistivity Logging-While-Drilling (LWD) Measurements Using a Self-Adaptive Goal-Oriented hp-Finite Element Method. *SIAM Journal on Applied Mathematics*, 66, pp. 2085-2106

Pardo, D. Calo, V. M. Torres-Verdin, C. Nam, M. J. (2008a) Fourier Series Expansion in a Non-Orthogonal System of Coordinates for Simulation of 3D DC Borehole Resistivity Measurements. *Computer Methods in Applied Mechanics and Engineering*, 197, 1-3, pp. 1906-1925

Pardo, D. Torres-Verdin, C. Nam, M. J. Paszyński, M.,. Calo, V. (2008b) Fourier Series Expansion in a Non-Orthogonal System of Coordinates for the Simulation of 3D Alternating Current Borehole Resistivity Measurements. *Computer Methods in Applied Mechanics and Engineering*, 197, 45-48, pp. 3836-3849

Kołodziej, J. Schaefer, R. Paszynska, A. (2004) Hierarchical genetic computation in optimal design, *Journal of Theoretical and Applied Mechanics*, 42 (3) pp.519–539

Schaefer, R., Kołodziej, J. (2003) Genetic search reinforced by the population hierarchy. In: *Foundations of Genetic Algorithms* 7, Morgan Kaufman Publisher, pp. 383–399.

Schaefer, R., Telega, H. (2007). Foundations of global genetic optimization. Heidelberg: Springer.